Published in final edited form as:
Trends Neurosci. 2014 August ; 37(8): 443–454. doi:10.1016/j.tins.2014.05.005.

From Molecule to Mind: an Integrative Perspective on Odor Intensity

Joel D. Mainland[1,2], **Johan N. Lundström**[1,3,4], **Johannes Reisert**[1], and **Graeme Lowe**[1]

[1]Monell Chemical Senses Center, PA, USA

[2]Department of Neuroscience, University of Pennsylvania, PA, USA

[3]Department of Clinical Neuroscience, Karolinska Institutet, Stockholm, Sweden

[4]Department of Psychology, University of Pennsylvania, PA, USA

Abstract

A fundamental problem in systems neuroscience is mapping the physical properties of a stimulus to perceptual characteristics. In vision, wavelength translates into color; in audition, frequency translates into pitch. Although odorant concentration is a key feature of olfactory stimuli, we do not know how concentration is translated into perceived intensity by the olfactory system. A variety of neural responses at several levels of processing have been reported to vary with odorant concentration, suggesting specific coding models. However, it remains unclear which, if any, of these phenomena underlie the perception of odor intensity. Here we provide an overview of current models at different stages of olfactory processing, and identify promising avenues for future research.

Introduction

> "I want to create a cologne that smells like a whisper. It'll be for all the secret admirers out there."
>
> – Jarod Kintz

Some odors whisper like a secret admirer, others blare like a megaphone. How does the brain encode such a broad spectrum of olfactory intensities? The majority of research in the field has focused on concentration, rather than intensity. While the intensity of an odorant is clearly related to its concentration [1], odorant concentration also correlates with odor valence [2], and quality [3]. Disentangling these perceptual dimensions is essential to understanding how intensity is encoded. This is particularly difficult in non-human model systems, where the neural code is most accessible, due to the inherent challenges of determining if a mouse has sensed a molecule's odor quality shift, e.g. from floral to fecal at

Corresponding author: Mainland, JD (jmainland@monell.org).

higher concentrations. Recent work suggests, however, that rats use a single intensity scale to discriminate concentrations of different odors [4] and points the way forward for examining intensity perception in animal models by dissociating concentration from intensity. Similarly, human lesion studies that suggest intensity and quality judgments are localizable to anatomically separate areas; lesions to the medial temporal lobe, formed by either resection or reoccurring epileptic activity, impair humans' ability to assess the identity or quality of odors, while leaving the ability to detect odors and perform odor intensity scaling tasks intact [5, 6]. Together, these results suggest that there is a common neural representation underlying intensity perception.

Several recent models have attempted to explain intensity coding at different levels in the olfactory system. Here we trace candidate intensity codes through ascending neural pathways from odor molecule detection by olfactory sensory neurons (OSNs) to signal integration in the olfactory bulb and processing in higher brain areas, focusing on mammalian model systems unless otherwise stated (Box 1). These models of intensity coding are speculative and we still lack a basic understanding of how odor intensity percepts are formed. It is our hope that this review can provide a useful overview of current thinking about a fundamental perceptual dimension of the sense of smell, and suggest further avenues of research. In the near future, we expect that technical innovations in imaging and optogenetics will enable the field to better test various hypotheses about intensity coding.

Box 1

Major ascending neural pathways in the mammalian olfactory system

Sensory pathways in the main olfactory system of mammals are illustrated for mouse (upper) and human (lower), two species in which odor intensity coding has been investigated (Figure I). Airborne odorants, drawn into nasal passages by phasic sniffing, adsorb to mucosal surfaces lining the main olfactory epithelium (*MOE*) and septal organ (*SO*, present in many non-human mammals). Odorant molecules are detected by olfactory sensory neurons (*OSNs*) that send primary afferents to the main olfactory bulb (*MOB*). Each OSN expresses a single type of olfactory receptor chosen from a large family of ~10^2 – 10^3 receptor genes. All OSNs expressing the same receptor send convergent projections to a few discrete glomeruli in the bulb, such that activated sets of glomeruli form stereotypic spatial maps (see also Fig. 4). Each glomerulus integrates afferent signals from thousands of OSNs, and relays output via a several dozen mitral/tufted cells. Mitral/tufted projections are distributed via the lateral olfactory tract (*LOT*) to a heterogeneous assemblage of secondary structures collectively labeled as olfactory cortex. Major recipients of bulb input include piriform cortex (*PC*) with anterior (*APC*) and posterior (*PPC*) subdivisions, and the anterior and posterolateral cortical amygdala (*Am*). Diffuse odor maps and widespread association fibers in the PC suggest a role in olfactory perceptual learning, whereas stereotypic projections to the amygdala may mediate innate odor driven behaviors. From here, odor information is routed to tertiary centers [113, 114] with the caudal orbitofrontal cortex (OFC) receiving the majority of projections from the piriform cortex [113]. The OFC is an important tertiary center receiving a majority of projections from the piriform cortex [113] and has been

implicated in odor identification, discrimination and memory. Other abbreviations: *AO*: anterior olfactory nucleus; *EC*: entorhinal cortex; *LOT*: lateral olfactory tract; *nLOT*: nucleus of the lateral olfactory tract; *Tu*: olfactory tubercle.

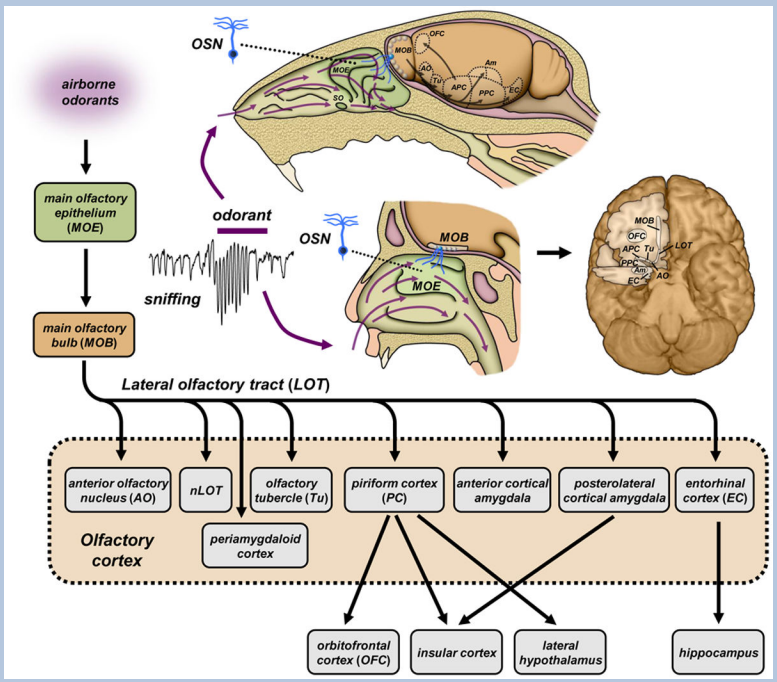

Figure I.

Intensity-concentration relationship

Empirically, the perceived intensity of an odorant is a monotonic, sigmoidal function of the logarithm of odorant concentration, although most early observations captured only the linear portion over a middle range of concentrations. In fact, many odorants fail to attain sufficiently high vapor concentrations to saturate the psychophysical function [7], so linear [8] and exponential [9] functions can indeed approximate the intensity-concentration function. However, a comparison of models found that the Hill equation is the most suitable model for a wide variety of odorants [1]:

$$I = I_{max} * C^n / (K^n + C^n)$$

where I_{max} is maximal odor intensity, C the odorant concentration, K the concentration at the inflection point on the log axis, and n the Hill exponent. Since the Hill exponent varies between odors, intensity is not an intrinsic property of an odorant. It is common to state, for example, that furfuryl mercaptan is “more intense” than vanillin. However, intensity is not an innate property of an odorant – one odor may be more intense than another at one concentration, but the reverse may be true at another concentration. For example, vanillin is detected at a lower concentration than cis-3-hexen-1-ol, but the latter is more intense at most suprathreshold concentrations [10].

Predicting odor intensity from chemical structure

There is currently no general model predicting the psychophysical intensity function from chemical structure. Certain physicochemical properties of molecules tend to be associated with high-potency odorants, such as high volatility and intermediate water-lipid partitioning, but odor intensity still spans several orders of magnitude for compounds with similar volatility and hydrophobicity.

General models *have* emerged for a special case of the psychophysical function relating concentration to intensity, namely the detection threshold [11, 12]. Accounting only for the transfer of odorants from gas phase to the mucosa – ignoring all receptor properties – these models are able to explain 76% of the variance in detection thresholds. Note, however, that this performance was measured on the training set and the model performance on a validation set may be lower. While receptor sensitivities still play a major role in detection thresholds [13], the receptor array appears to be generally capable of detecting the majority of molecules that can be transported to the mucosa. These solvation models apply to only one point on the concentration-intensity function and the rank order of odors by threshold does not necessarily predict the rank order of perceived intensity at higher concentrations. Although there have been efforts to predict suprathreshold intensity from molecular properties [14], a formal model has yet to be developed.

Neural encoding – predicting odor intensity from spike patterns

Chemical signals detected by odorant receptors in OSNs are transformed into sequences of action potentials or spikes relayed to the brain. Spikes are digital signals whose number, timing and distribution across neural assemblies contain all of the stimulus information available to the nervous system. A variety of schemes have been proposed for spike encoding of odor intensity at different stages in the olfactory pathway, based on observing changes in neural activity as a function of odorant concentration.

Olfactory sensory neurons

When odorants bind olfactory receptors in OSNs, they initiate a series of intracellular events producing second-messenger signals that gate ion channels. These transduction channels conduct a depolarizing current that drives spike firing (see Fig. 1). Low channel noise facilitates reliable high-gain amplification of weak signals[15], and high input resistance of OSNs confers high sensitivity, with spike responses being elicited by small currents of only a few pA, or even single ion channel openings [16–18]. In the absence of odor stimuli, basal firing of OSNs is low (0.05 –3 Hz) [19–21]. Odorants elevate the firing rate and total number of spikes fired increases up to intermediate concentrations, but can then drop to only 2 –3 spikes at saturating concentrations. With firing frequencies as high as 200 Hz and only a few spikes, response duration can be as short as 10 –15 ms. In addition, latency from stimulus onset to first spike becomes shorter in proportion to logarithm of concentration, with latency at high concentrations as short as 30 ms [22, 23]. Thus, at the level of the primary sensory neurons, odorant concentration could be encoded in spike frequency, number of spikes generated, and/or latency to first spike (Fig. 1).

Olfactory bulb

Afferent fibers of OSNs arriving at the olfactory bulb are routed to discrete glomeruli according to their expression of one of ~10^2 –10^3 types of different olfactory receptors. Thus, each glomerulus receives OSN input arising from many copies of a single type of olfactory receptor distributed throughout the olfactory epithelium. Previous functional analysis of ORs showed that different odorants are recognized by unique, but overlapping ensembles of ORs [24, 25], suggesting a combinatorial code for odor quality. OSN inputs are spread across multiple glomerular channels arranged in stereotypic spatial maps of receptor identity. When these input maps are visualized directly by presynaptic calcium imaging of OSN terminals [26], both increased magnitude and decreased latency of glomerular responses are seen at higher odorant concentrations [27], consistent with response properties of OSNs. These shifts occur independently in each glomerulus and hence provide an analytic representation of the intensities of an odorant detected by each type of receptor. Magnitudes of glomerular presynaptic signals have wider dynamic ranges (> 2 log units concentration) than single OSN spike responses (~1 –2 log units). This may reflect variable odorant sensitivity in populations of OSNs expressing the same receptor, which would serve to expand the concentration ranges of glomerular intensity codes [28, 29]. Within the bulb, input signals received by glomeruli activate several layers of excitatory and inhibitory circuitry to shape the spike patterns of mitral/ tufted cells relaying bulb output to olfactory cortical centers. A recent study took advantage of optogenetic techniques to show that mice are able to perceive a variety of neural activity features at the level of OSN input to the glomerulus [30]. In this study, mice could distinguish if a single glomerulus was activated or not, even against a background odor. They could also distinguish between different amplitudes of single-glomerular activation, and input timing differences as small as 25 ms. Thus, all of these features are plausible as perceptually relevant sources of information about the odor stimulus. Which features represent odor intensity, and which represent other information, such as odor quality?

We consider several models of odor intensity coding at this level. Are they compatible with physiological data? Do they predict stable perception of odor quality over a range of concentrations? Although the neural code in the olfactory bulb must represent both odor concentration and quality, it is crucial for the brain to disambiguate the two kinds of information. For olfactory navigation tasks, stimulus concentration varies with distance from a target odor source; animals must be able to maintain a concentration-invariant representation of odor quality over biologically-relevant concentration ranges to track the source. Although odors are generally thought to retain their quality over a range of concentrations, concentration changes greater than two orders of magnitude may yield changes in odor quality for some odorants [3, 31] but not others [32].

Spike rate coding

Since odorant concentration is correlated with spike rates of OSN inputs to glomeruli, we may ask if this rate code is copied by synaptic excitation to ensembles of mitral/ tufted cells linked to these glomeruli. Such a scheme allows a straightforward coding of intensity (as firing rate) while maintaining concentration invariance of the odor quality code (as pattern of active glomeruli). However, it may be incompatible with widespread synaptic inhibition

in bulb circuits. Indeed, although some mitral/tufted cells do respond to odor stimuli with increased spike excitation at higher odorant concentration, others are inhibited, or respond with more complex temporal patterns of mixed excitation and inhibition that may change with concentration. This variability in responses was first observed in rodents using odorant stimuli delivered to anesthetized animals by steady airflow [33, 34], and was confirmed in both anesthetized and awake animals under more natural periodic stimulation or sniffing [35–37]. Inhaled odorants elicit sniff-locked rhythmic spike bursting and/ or spike inhibition with a diverse phase distribution over the sniff cycle. Cells that display immediate excitatory responses could selectively convey rate codes of intensity. However, cells that are excited by some odorants may be inhibited by other odorants via lateral inhibition, complicating the readout. In awake rodents, mitral/tufted cells have a high mean rates of spontaneous discharge (~ 30 Hz) [38], which would reduce the available dynamic range for elevations in spike rate, while increasing it for suppression. Furthermore, mitral cell membrane biophysics favors a resonant frequency of ~ 40 Hz for intraburst firing rates [39], and the rates are not very sensitive to odorant concentration [40, 41].

Spike latency coding

Glomerular inputs also carry a latency code of odorant concentration that could be transferred to bulb neurons [27]. Indeed, at higher odorant concentration spike latencies of mitral cell excitatory responses are clearly reduced [41]. If these reductions occur uniformly across inputs, then patterns of relative latency between glomeruli could act as concentration-invariant codes for odor quality (Fig. 2) [42–44]. This scheme can account for fast discrimination of odors in single sniffs < 200 ms in duration. As in rate models, coding may be complicated by lateral inhibition. Stronger sensory input can increase spike latency in some mitral cells by strengthening inhibition, which would violate pattern invariance. This could be resolved by prioritizing readout of the code to emphasize earlier excitatory responses that only show latency reductions. Lateral inhibition could sharpen this temporal window of readout by allowing earlier stronger responses to delay or block later, weaker responses [43]. High spontaneous firing of mitral/tufted cells in awake animals also poses a problem for latency coding. In more active cells, the first spike of a response is harder to distinguish from background spikes and firing must be analyzed over finite time windows, repeated sniff cycles, or across many cells of an ensemble to identify responses and measure latencies. The first two strategies would tend to negate the speed advantage of latency coding.

Latency coding models require a reference time frame to compute spike delays. The periodic inhalation cycle of sniffing was suggested to serve this purpose. This may work in small animals like mice whose short sniff cycles (< 200 ms) may sample odor stimuli in discrete packets. However, in larger species with slower sniff rates there may be variability in odorant arrival time at the olfactory epithelium during a sniff, which would cause errors in latency. Timing signals directly locked to odorant stimulation would be more reliable. Such signals may be generated in each glomerulus by the tufted cells, which receive direct monosynaptic excitation from OSNs [45] and respond to odorants with short latencies nearly independent of concentration. In contrast, mitral cells receive polysynaptic excitation via external tufted (ET) cells [45] and have longer latencies that decrease with increasing

concentration [46]. Thus, the relative sniff phase of responses of ‘sister’ mitral and tufted cells connected to the same glomerulus could encode intensity for each glomerular channel (Fig. 3C). Tufted cells receive less lateral inhibition than mitral cells, have lower firing thresholds, and their odorant responses span a much broader range of spike frequencies (< ~400 Hz) [47], and they could transmit a parallel rate code of concentration.

Recently, a novel latency-coding model was proposed based on a different stimulus-locked timing signal. In rodents, each olfactory receptor is mapped to a pair of glomeruli, located in the medial and lateral halves of the bulb. These glomeruli receive inputs from OSNs in medial and lateral regions of the nasal cavity, respectively [48]. Inhaled odorants are transported more rapidly to medial OSNs, and mitral cells connected to medial glomeruli have shorter latency responses that can be used for timing reference. Slower penetration of odorants into lateral recesses of the nasal cavity increases the relative latencies of lateral glomerulus mitral cells by ~ 60 ms [49]. These medio-lateral timing differences are systematically decreased at higher odorant concentrations, and could therefore be utilized for receptor-specific intensity coding (Fig. 3D–E). Optogenetic stimulation of multiple glomeruli has shown that downstream neurons in piriform cortex may able to read this kind of temporal code. Cortical neurons were sensitive to interglomerular optical stimulus delays in the range ~0 –50 ms, which is well matched to medio-lateral delays, and could discriminate the order of activation[50].

Thus far we have discussed analytic representations of intensity divided among many glomerular data channels. However, our odor perceptions are largely synthetic and expressed in terms of odor ‘objects’ constructed at higher cortical levels (e.g. the smell of ‘rose’ or ‘coffee’). We attach to an odor object a single intensity value rather than hundreds of low-level intensity codes of receptors and glomeruli. A fundamental problem then is to determine where and how a single intensity is computed. Some models have proposed that overall odor intensity may already be encoded in the olfactory bulb.

Spatial extent coding

An increase in odorant concentration is accompanied by an increase in the number of types of activated receptors [24, 51] and OSNs [52], and a corresponding expansion of presynaptic activity maps due to recruitment of additional glomerular inputs detected by imaging in anesthetized animals [26, 53] (Fig. 4). Glomerular recruitment was also detected by other measurements of glomerular response with postsynaptic signal components [54–56], and also occurs in awak animals [57]. The recruitment rate roughly matches the Weber ratio of just noticeable relative concentration change in humans [58], suggesting that the total number of activated glomeruli, or spatial extent of bulb activity, may constitute an ensemble code for intensity. Assuming that odor quality is encoded by a glomerular identity code, a large change in spatial extent could potentially confuse odor intensity and quality codes. However, awake rats were shown to recognize stable odor percepts as the extent of glomerular input maps varied greatly with concentration [59]. A few studies have reported relative stability in patterns of active glomeruli across concentrations. This might be due to differences in sensitivity or thresholding of detected signals (fMRI), or variation in olfactory receptor tuning between species (turtle) [60, 61].

Glomerular recruitment has thus far only been documented in anesthetized preparations. Awake animals might be able to adjust sniffing rate and depth to stabilize glomerular representations as concentration is increased. Concentration invariance could also be achieved by postsynaptic processing in the bulb. Computer models have predicted that wide-ranging recurrent excitation of short axon (SA) cells that connect many glomeruli, in conjunction with mitral/ tufted cell inhibition by periglomerular cells, may normalize postsynaptic spatial activity patterns evoked by different odorant concentrations [62]. In the process, SA networks would compute a global mean strength of input that might serve as a single readout of stimulus intensity. Such computations are implemented in zebrafish bulb by an interneuron network that uses electrical coupling to boost weak responses and GABAergic inhibition to attenuate strong responses [63]. However, this normalization mechanism does not seem to operate in the mouse, because glomerular recruitment is still detectable postsynaptically in patterns of mitral/ tufted cell response mapped by GCaMP2 imaging of calcium in dendritic tufts [64]. Perceptual invariance may rely on processing and decoding of mitral/ tufted cell spike outputs at the ensemble level. During each sniff cycle, multielectrode recordings in anesthetized mice reveal shifting patterns of odor-evoked activity sweeping through mitral cell populations. The dynamics are odorant-specific and their trajectories are clustered more coarsely by odorant, and more finely by concentration, and thus permit a separation of quality vs. intensity (Bathellier & al 2008). Similar separation of odor intensity vs. quality by ensemble dynamics is observed in widely differing species, e.g. zebrafish mitral cells [65] and locust antennal lobe projection neurons (Stopfer & al 2003 Neuron, 39: 991; Shen et al 2013 Neuron 80: 1–17). Zebrafish bulb circuits also appear to be wired so that time-dependent decorrelation of input patterns selectively amplifies differences between patterns evoked by different odorants, but not those evoked by the same odorant at different concentrations [65]. In addition to this processing in the OB, downstream pattern completion networks in piriform cortex might be trained to recognize the same odor object even if glomerular response patterns vary with odorant concentration [66]. Spatial extent models of intensity coding might seem inconsistent with a recent study showing that mice can discriminate different stimulus intensities delivered optogenetically to a single glomerulus glomerulus [30]. However, it is not known if this optogenetic intensity is perceptually equivalent to odor intensity to these animals.

Coding by dedicated intensity channels

A family of broadly tuned low-affinity receptors have been hypothesized to function as simple intensity detectors [67]. The septal organ (Organ of Masera) is an isolated patch of olfactory epithelium expressing a small repertoire of less than a dozen odorant receptors in 95% of its OSNs [68]. One dominant receptor, SR1, occurring in ~50 % of OSNs in the septal organ, is very broadly tuned and may function as a general tranducer of concentration for a wide variety of odorants[69]. Cells expressing SR1 can respond to odorant concentrations spanning 4 log units, a 100-fold greater range than many other OSNs. Although this is still much less than psychophysical dynamic ranges of olfaction (e.g. ~ 6 log units for humans, ~10 for dogs), it may be sufficient to encode intensity for a subset of odorants over biologically relevant concentration ranges. In the main olfactory epithelium there are additional broadly tuned receptors detecting other classes of odorants [25].

Together these could cover a wider range of concentrations and encode intensity for many more odorants. This model implies the existence of broadly tuned glomeruli with specialized projections for conveying intensity information. The septal organ projects heavily to a few glomeruli in the posterior, ventromedial area of the main olfactory bulb [70]. It will be interesting to see if mice with genetic disruption [71] or lesions of these glomeruli can learn odor intensity discriminations. Dedicated intensity readouts may help regulate low-level sensory mechanisms independent of conscious perception of stimulus intensity in higher brain centers. For example, in vision the pupillary light reflex at high light intensities is mediated by photosensitive melanopsin-expressing retinal ganglion cells [72]. One might imagine specialized pathways also exist for controlling olfactomotor reflexes [73].

The above models of intensity coding attempt to identify simple neural schemes based on observing and correlating responses with changing concentrations of a series of monomolecular odorant stimuli delivered in controlled laboratory settings. Although each has its strengths and weaknesses, there is currently insufficient data to clearly distinguish between them. Moreover, they provide little insight into how perceived intensity might vary for structurally diverse odorants presented in simple or complex mixtures, or when olfactory adaptation occurs in real world situations. A better understanding of these issues may require bridging the gap between low level analytic coding by receptors and glomeruli, and high level synthetic coding of odor objects in cortical areas.

Odor intensity from cortical activation

To date, few studies have directly assessed the central neural network responsible for the processing of perceived odor intensity or odor concentration. A major reason for this dearth of knowledge is the aforementioned inherently confounding co-dependency between the three perceptual odor dimensions intensity, valence, and quality. This interdependence among dimensions renders the task of isolating cognitive processing of intensity perception inherently difficult. Nonetheless, increased attention has lately been devoted to higher-order processing areas in animal and human models alike.

Intensity-dependent processing in the murine cortex

Odor representations in the murine piriform cortex (PC), one of the main components of primary olfactory cortex, differ profoundly from the stereotypic glomerular maps encoding odorant molecular features in the olfactory bulb. Calcium imaging revealed that odorant stimulation elicits diffuse activation of PC neural ensembles without clear spatial patterning [74]. Increasing odorant concentration recruited additional cells in a sub-linear manner, with at most 20% of PC cells activated at higher concentrations. Individual responses increased sublinearly in two thirds of cells, and decreased in the remaining third, suggesting engagement of inhibitory pathways. Recruitment of PC neurons is consistent with recruitment of additional receptors/ glomeruli in bulbar odor maps at higher concentrations. Glomeruli send diffuse overlapping mitral/ tufted projections across the PC [75–77] and PC pyramidal neuron responses are determined by threshold integration of excitatory inputs from multiple glomeruli [78–80]. Adding more glomeruli to bulbar maps is expected to bring more pyramidal neurons above threshold. Both the change in composition of the active PC ensemble, and its differential excitation/ inhibition, are possible encoders of stimulus

intensity. PC neurons are sensitive to timing differences of bulbar inputs, and may transform latency codes of mitral/ tufted cells into firing rate intensity codes [50]. Mitral cells have wide ranging projections to most of olfactory cortex, whereas tufted cells target more restricted rostral areas [76, 77]. These differences could map activation differences between mitral and tufted cells into concentration-dependent response patterns across PC neurons. Indeed, intrinsic optical imaging of dorsal anterior PC showed that increasing odorant concentration expands the area of cortical activation along the rostrocaudal axis [81, 82]. Single unit recordings revealed a gradient in response thresholds, with lower thresholds at the rostral end where tufted cells have more projections [81].

Intensity-dependent processing in the human cortex

Initial studies assessing cerebral processing of perceived odor intensity in humans using event-related potentials (ERP), derived from electroencephalography (EEG) recordings, demonstrated that odor intensity/concentration is negatively correlated with response latencies and positively correlated with response amplitudes in foremost the early perceptually-related components[83, 84]; i.e. a more intense odor is processed faster and produce stronger responses than a weaker odor. This is in accordance with the aforementioned data obtained in peripheral recordings from animal models. Although a method with superior temporal resolution, EEG/ERP studies have not been able to provide a deeper understanding of the underlying neural mechanisms due to the lack of reliable spatial information. More recently, studies assessing judgments of odor intensity employing fMRI, a method with better spatial resolution, have consistently indicated that areas within the temporal lobes, such as the entorhinal cortex (EC) [85, 86], the PC [85, 87], and the amygdala [88] correlate with odor intensity perception. Several of these studies employed a simple contrast between high and low intensity odors, which fails to dissociate intensity from a variety of confounding psychological constructs (e.g., valence and quality). Moreover, these areas are located within close proximity of each other and in most of these studies, activations occur in overlapping anatomical regions, thus rendering it difficult to define primary areas of processing. Subsequent studies employing analyses dependent on continuous relationships with the psychological intensity percept have, however, indicated that judgments of odor intensities are linearly correlated with activity within the PC [85] and demonstrated a dissociation between the temporal and frontal portion of the PC in an attention-dependent manner [89]. Early studies frequently implicated intensity-dependent processing within the caudal areas of the orbitofrontal cortex (OFC) [85, 87, 90]. More recent studies suggest, however, that the main role of these areas is to form the final conscious percept of odor quality [91–93] by acting as an integrator of convergent signals from olfactory and other sensory and cognitive systems [94–96]. Given the heterogeneous nature of many of the areas within the olfactory network and the likely dependency of multiple amodal neural networks, it is difficult to isolate processing of intensity from other cognitive or perceptual activities. Some studies have attempted to isolate intensity by including several qualities with a spread among the valence axis to factor out valence-dependent activity, but the cognitive processing of the odor quality may induce confounding activity unrelated to intensity processing, such as memory retrieval. For example, while the EC is commonly implicated in odor processing [97], recent studies suggest that the main

role of this structure in the temporal cortex is related to memory or identity retrieval rather than directly involved in odor intensity processing per se [98, 99].

In summary, these studies suggest that the PC is one of the key nodes in the neural network processing odor intensity judgments. The lack of significant involvement from higher order cognitive processing areas supports the view that basic intensity processing in the olfactory sense is to a large extent dependent on peripheral signal processing with rather limited cognitive modulation. However, studies assessing intensity processing in human participants are scarce and, due to methodological limitations, have yet to directly connect with more recent studies in animal models beyond mapping of cerebral processing areas.

How quickly is intensity computed?

In land-based vertebrates, olfactory perception begins with the inhalation (sniffing) of odorous air into the nasal cavity. A sniff begins with a stimulus-independent inhalation, but is rapidly modulated in response to sniff content. Sniffs of different odorant concentrations are uniform for the first 160–260 ms following sniff onset, but then diverge such that sniffs of a concentrated odorant will have a smaller volume than sniffs of a diluted odorant [73]. This relationship is sufficiently robust to serve as a non-verbal test of odorant detection [100]. Adding OSN response delays following onset of stimulation and efferent nasal airflow [22, 101, 102] yields an overall peripheral response delay of ~50 ms, which is roughly matched by the response delay of mitral cells in the bulb following the onset of inhalation [46, 103]. Several groups found that both rats and mice could perform simple odor discrimination tasks within a single sniff in less than 200 ms [104–106]. This suggests that the neural computation time for odor identification and decision making is on the time scale of 150 ms. The rapid adjustment of airflow in response to odor concentration implies that at least one representation of intensity is likely subcortical, as human olfactory cortical evoked potentials are not typically seen until 150 to 400 ms following stimulus onset [107–109].

Conclusion

The vast majority of olfactory stimuli encountered in nature are complex mixtures of odorant molecules. When the intensities of the component odorants are known, what is the intensity of the mixture? The intensity of an odorant mixture is rarely a simple linear sum of the intensities of individual components [110], but as noted above, non-linear models, such as the Hill equation, are often a better fit to the concentration-intensity relationship. Thus, mixture interactions that deviate from a linear sum of components may be an inherent property of the non-linear, sigmoidal psychophysical function, rather than interactions between the odorants at the receptor level. Indeed, work at the glomerular level failed to find any results that did not fit a simple competitive binding model [111]. Due to the current lack of a model for predicting the intensity of a complex mixture, standard practice for determining the intensity of a mixture in regulatory agencies and industrial settings is to use a human sensory panel trained in the use of a dynamic-dilution olfactometer.

A major obstacle in the field has been the inability to assess perceived intensity in animal models. Training animals to perform a concentration-discrimination task is straightforward; obtaining an accurate readout of perceived intensity is not. This has led the majority of researchers to base their models on concentration and focus on within-odor manipulations where concentration and intensity changes are closely related. To distinguish between the models reviewed here, future experiments must dissociate concentration from intensity. A valid model of intensity perception must be able to predict intensity across odors, as odors are mixed, and as adaptation occurs. For example, which neural feature is consistent across stimulation with the 144 odors that have been intensity-balanced in humans [112] or the 12 odor pairs that have been intensity-balanced in rats [4]? In rats, adaptation to an odor for 300 ms was perceived as equivalent in intensity to a 3- to 10-fold dilution of the odor [4]. Which neural feature is consistent across the diluted and adapted stimuli? In addition, a model of intensity must disentangle confounding factors such as odorant quality and valence.

Acknowledgments

JM is supported by NIH grant DC013339. JNL is supported by the Knut and Alice Wallenberg Foundation (KAW 2012.0141). JR is supported by NIH grant DC009613. GL is supported by NIH grant DC04208.

Glossary

Lateral inhibition	the process whereby an excited neuron reduces the activity of parallel neurons through inhibitory synaptic connections. In the olfactory bulb, parallel mitral/ tufted cells affiliated with different glomeruli can laterally inhibit each via local interneuron circuits composed of periglomerular, short axon or granule cells
Presynaptic calcium imaging	a method for optical detection of neural activity based on localizing a fluorescent calcium-sensitive probes into presynaptic nerve terminals. In the olfactory system, synthetic dextran-conjugated calcium indicator dyes are loaded into OSNs by intranasal perfusion, and are transported through axons to ON terminals in glomeruli. This allows visualization of odor-encoding glomerular activity maps by fluorescent imaging. The method is also implemented by driving expression of a genetically encoded calcium indicator (e.g. GCaMP2) in OSNs using a promoter for olfactory marker protein (OMP), which is expressed in all mature OSNs
GCaMP2 imaging	GCaMP2, a genetically encoded reporter protein whose fluorescence increases as intracellular calcium levels rise when neurons fire action potentials. In the olfactory system, mouse strains expressing GCaMP2 in OSNs, and in mitral/ tufted cells, have been used to map patterns of glomerular activity encoding different odorants
Amodal neural network	A network that is not primarily dedicated to the processing of information from a specific sensory modality, such as vision, audition, or olfaction

References

1. Chastrette M, et al. Modelling the human olfactory stimulus-response function. Chem Senses. 1998; 23:181–196. [PubMed: 9589166]
2. Henion KE. Odor pleasantness and intensity: a single dimension? J Exp Psychol. 1971; 90:275–279. [PubMed: 5134332]
3. Gross-Isseroff R, Lancet D. Concentration-dependent changes of perceived odor quality. Chem Senses. 1988; 13:191.
4. Wojcik PT, Sirotin YB. Single scale for odor intensity in rat olfaction. Current biology : CB. 2014; 24:568–573. [PubMed: 24560575]
5. Eichenbaum H, et al. Selective olfactory deficits in case H.M. Brain. 1983; 106 (Pt 2):459–472. [PubMed: 6850278]
6. Jones-Gotman M, Zatorre RJ. Olfactory identification deficits in patients with focal cerebral excision. Neuropsychologia. 1988; 26:387–400. [PubMed: 3374800]
7. Moskowitz HR, et al. Odor intensity and pleasantness for a diverse set of odorants. Perception and Psychophysiology. 1976:122–128.
8. Fechner, GT. Elemente der Psychophysik. Breitkopf & Härtel; 1860.
9. Stevens SS. On the psychophysical law. Psychol Rev. 1957; 64:153–181. [PubMed: 13441853]
10. Valérie, A., et al. Limitations in the Use of Odor Activity Values to Determine Important Odorants in Foods. In: Leland, JV., et al., editors. Gas Chromatography--Olfactometry. 2001. p. 156-171.
11. Abraham MH, et al. An algorithm for 353 odor detection thresholds in humans. Chem Senses. 2012; 37:207–218. [PubMed: 21976369]
12. Hau KM, Connell DW. Quantitative Structure-Activity Relationships (QSARs) for Odor Thresholds of Volatile Organic Compounds (VOCs). Indoor Air. 1998; 8:23–33.
13. Keller A, et al. Genetic variation in a human odorant receptor alters odour perception. Nature. 2007; 449:468–472. [PubMed: 17873857]
14. Cain WS. Odor intensity: Differences in the exponent of the psychophysical function. Attention, Perception, & Psychophysics. 1969; 6:349–354.
15. Kleene SJ. High-gain, low-noise amplification in olfactory transduction. Biophysical Journal. 1997; 73:1110–1117. [PubMed: 9251827]
16. Maue RA, Dionne VE. Patch-clamp studies of isolated mouse olfactory receptor neurons. Journal of General Physiology. 1987; 90:95–125. [PubMed: 2442298]
17. Lynch JW, Barry PH. Action potentials initiated by single channels opening in a small neuron (rat olfactory receptor). Biophysical Journal. 1989; 55:755–768. [PubMed: 2470428]
18. Reisert J, Matthews HR. Adaptation of the odour-induced response in frog olfactory receptor cells. Journal of Physiology-London. 1999; 519:801–813.
19. O'Connell RJ, Mozell MM. Quantitative stimulation of frog olfactory receptors. Journal of Neurophysiology. 1969; 32:51–63. [PubMed: 5765230]
20. Reisert J. Origin of basal activity in mammalian olfactory receptor neurons. J Gen Physiol. 2010; 136:529–540. [PubMed: 20974772]
21. Duchamp-Viret P, et al. Peripheral odor coding in the rat and frog: Quality and intensity specification. Journal of Neuroscience. 2000; 20:2383–2390. [PubMed: 10704512]
22. Ghatpande AS, Reisert J. Olfactory receptor neuron responses coding for rapid odour sampling. The Journal of physiology. 2011; 589:2261–2273. [PubMed: 21486768]
23. Rospars JP, et al. Spiking frequency versus odorant concentration in olfactory receptor neurons. Biosystems. 2000; 58:133–141. [PubMed: 11164640]
24. Malnic B, et al. Combinatorial receptor codes for odors. Cell. 1999; 96:713–723. [PubMed: 10089886]
25. Nara K, et al. A large-scale analysis of odor coding in the olfactory epithelium. The Journal of neuroscience. 2011; 31:9179–9191. [PubMed: 21697369]
26. Wachowiak M, Cohen LB. Representation of odorants by receptor neuron input to the mouse olfactory bulb. Neuron. 2001; 32:723–735. [PubMed: 11719211]

27. Spors H, et al. Temporal dynamics and latency patterns of receptor neuron input to the olfactory bulb. The Journal of neuroscience : the official journal of the Society for Neuroscience. 2006; 26:1247–1259. [PubMed: 16436612]
28. Bozza T, et al. Odorant receptor expression defines functional units in the mouse olfactory system. J Neurosci. 2002; 22:3033–3043. [PubMed: 11943806]
29. Grosmaitre X, et al. Odorant responses of olfactory sensory neurons expressing the odorant receptor MOR23: a patch clamp analysis in gene-targeted mice. Proc Natl Acad Sci U S A. 2006; 103:1970–1975. [PubMed: 16446455]
30. Smear M, et al. 2013Multiple perceptible signals from a single olfactory glomerulus. Nat Neurosci.
31. Laing DG, et al. Relationship between molecular structure, concentration and odor qualities of oxygenated aliphatic molecules. Chem Senses. 2003; 28:57–69. [PubMed: 12502524]
32. Krone D, et al. Qualitative and quantitative olfactometric evaluation of different concentrations of ethanol peppermint oil solutions. Phytotherapy research : PTR. 2001; 15:135–138. [PubMed: 11268113]
33. Mair RG. Adaptation of rat olfactory bulb neurones. J Physiol. 1982; 326:361–369. [PubMed: 7108800]
34. Meredith M. Patterned response to odor in mammalian olfactory bulb: the influence of intensity. J Neurophysiol. 1986; 56:572–597. [PubMed: 3537224]
35. Wellis DP, et al. Discrimination among Odorants by Single Neurons of the Rat Olfactory-Bulb. J Neurophysiol. 1989; 61:1161–1177. [PubMed: 2746317]
36. Bathellier B, et al. Dynamic ensemble odor coding in the mammalian olfactory bulb: sensory information at different timescales. Neuron. 2008; 57:586–598. [PubMed: 18304487]
37. Cury KM, Uchida N. Robust odor coding via inhalation-coupled transient activity in the mammalian olfactory bulb. Neuron. 2010; 68:570–585. [PubMed: 21040855]
38. Rinberg D, et al. Sparse odor coding in awake behaving mice. The Journal of neuroscience : the official journal of the Society for Neuroscience. 2006; 26:8857–8865. [PubMed: 16928875]
39. Desmaisons D, et al. Control of action potential timing by intrinsic subthreshold oscillations in olfactory bulb output neurons. The Journal of neuroscience : the official journal of the Society for Neuroscience. 1999; 19:10727–10737. [PubMed: 10594056]
40. Chalansonnet M, Chaput MA. Olfactory bulb output cell temporal response patterns to increasing odor concentrations in freely breathing rats. Chem Senses. 1998; 23:1–9. [PubMed: 9530964]
41. Cang J, Isaacson JS. In vivo whole-cell recording of odor-evoked synaptic transmission in the rat olfactory bulb. The Journal of neuroscience : the official journal of the Society for Neuroscience. 2003; 23:4108–4116. [PubMed: 12764098]
42. Hopfield JJ. Pattern-Recognition Computation Using Action-Potential Timing for Stimulus Representation. Nature. 1995; 376:33–36. [PubMed: 7596429]
43. Schaefer AT, Margrie TW. Spatiotemporal representations in the olfactory system. Trends Neurosci. 2007; 30:92–100. [PubMed: 17224191]
44. Schaefer AT, Margrie TW. Psychophysical properties of odor processing can be quantitatively described by relative action potential latency patterns in mitral and tufted cells. Frontiers in systems neuroscience. 2012; 6:30. [PubMed: 22582039]
45. Gire DH, et al. Mitral cells in the olfactory bulb are mainly excited through a multistep signaling path. The Journal of neuroscience : the official journal of the Society for Neuroscience. 2012; 32:2964–2975. [PubMed: 22378870]
46. Fukunaga I, et al. Two distinct channels of olfactory bulb output. Neuron. 2012; 75:320–329. [PubMed: 22841316]
47. Nagayama S, et al. Mitral and tufted cells differ in the decoding manner of odor maps in the rat olfactory bulb. J Neurophysiol. 2004; 91:2532–2540. [PubMed: 14960563]
48. Schoenfeld TA, Cleland TA. The anatomical logic of smell. Trends Neurosci. 2005; 28:620–627. [PubMed: 16182387]
49. Zhou Z, Belluscio L. Coding odorant concentration through activation timing between the medial and lateral olfactory bulb. Cell reports. 2012; 2:1143–1150. [PubMed: 23168258]

50. Haddad R, et al. Olfactory cortical neurons read out a relative time code in the olfactory bulb. Nat Neurosci. 2013; 16:949–957. [PubMed: 23685720]
51. Kajiya K, et al. Molecular bases of odor discrimination: Reconstitution of olfactory receptors that recognize overlapping sets of odorants. J Neurosci. 2001; 21:6018–6025. [PubMed: 11487625]
52. Ma M, Shepherd GM. Functional mosaic organization of mouse olfactory receptor neurons. Proc Natl Acad Sci U S A. 2000; 97:12869–12874. [PubMed: 11050155]
53. Bozza T, et al. In vivo imaging of neuronal activity by targeted expression of a genetically encoded probe in the mouse. Neuron. 2004; 42:9–21. [PubMed: 15066261]
54. Rubin BD, Katz LC. Optical imaging of odorant representations in the mammalian olfactory bulb. Neuron. 1999; 23:499–511. [PubMed: 10433262]
55. Meister M, Bonhoeffer T. Tuning and topography in an odor map on the rat olfactory bulb. J Neurosci. 2001; 21:1351–1360. [PubMed: 11160406]
56. Spors H, Grinvald A. Spatio-temporal dynamics of odor representations in the mammalian olfactory bulb. Neuron. 2002; 34:301–315. [PubMed: 11970871]
57. Vincis R, et al. Dense representation of natural odorants in the mouse olfactory bulb. Nat Neurosci. 2012; 15:537–539. [PubMed: 22406552]
58. Koulakov A, et al. Olfactory coding with all-or-nothing glomeruli. J Neurophysiol. 2007; 98:3134–3142. [PubMed: 17855585]
59. Homma R, et al. Perceptual stability during dramatic changes in olfactory bulb activation maps and dramatic declines in activation amplitudes. The European journal of neuroscience. 2009; 29:1027–1034. [PubMed: 19291227]
60. Xu F, et al. Assessment and discrimination of odor stimuli in rat olfactory bulb by dynamic functional MRI. Proc Natl Acad Sci U S A. 2000; 97:10601–10606. [PubMed: 10973488]
61. Wachowiak M, et al. Distributed and concentration-invariant spatial representations of odorants by receptor neuron input to the turtle olfactory bulb. J Neurophysiol. 2002; 87:1035–1045. [PubMed: 11826067]
62. Cleland TA, et al. Relational representation in the olfactory system. Proc Natl Acad Sci U S A. 2007; 104:1953–1958. [PubMed: 17261800]
63. Zhu P, et al. Equalization of odor representations by a network of electrically coupled inhibitory interneurons. Nat Neurosci. 2013
64. Fletcher ML, et al. Optical imaging of postsynaptic odor representation in the glomerular layer of the mouse olfactory bulb. J Neurophysiol. 2009; 102:817–830. [PubMed: 19474178]
65. Niessing J, Friedrich RW. Olfactory pattern classification by discrete neuronal network states. Nature. 2010; 465:47–52. [PubMed: 20393466]
66. Wilson DA. Pattern separation and completion in olfaction. Ann N Y Acad Sci. 2009; 1170:306–312. [PubMed: 19686152]
67. Firestein S. How the olfactory system makes sense of scents. Nature. 2001; 413:211–218. [PubMed: 11557990]
68. Ma, M. Multiple Olfactory Subsystems Convey Various Sensory Signals. In: Menini, A., editor. The Neurobiology of Olfaction. 2010.
69. Grosmaitre X, et al. SR1, a mouse odorant receptor with an unusually broad response profile. The Journal of neuroscience. 2009; 29:14545–14552. [PubMed: 19923288]
70. Levai O, Strotmann J. Projection pattern of nerve fibers from the septal organ: DiI-tracing studies with transgenic OMP mice. Histochem Cell Biol. 2003; 120:483–492. [PubMed: 14628145]
71. Fuss SH, et al. Odorant receptor gene choice and axonal wiring in mice with deletion mutations in the odorant receptor gene SR1. Molecular and Cellular Neuroscience. 2013
72. Do MT, Yau KW. Intrinsically photosensitive retinal ganglion cells. Physiol Rev. 2010; 90:1547–1581. [PubMed: 20959623]
73. Johnson BN, et al. Rapid olfactory processing implicates subcortical control of an olfactomotor system. J Neurophysiol. 2003; 90:1084–1094. [PubMed: 12711718]
74. Stettler DD, Axel R. Representations of odor in the piriform cortex. Neuron. 2009; 63:854–864. [PubMed: 19778513]

75. Sosulski DL, et al. Distinct representations of olfactory information in different cortical centres. Nature. 2011; 472:213–216. [PubMed: 21451525]
76. Igarashi KM, et al. Parallel mitral and tufted cell pathways route distinct odor information to different targets in the olfactory cortex. The Journal of neuroscience. 2012; 32:7970–7985. [PubMed: 22674272]
77. Nagayama S, et al. Differential axonal projection of mitral and tufted cells in the mouse main olfactory system. Frontiers in neural circuits. 2010; 4
78. Apicella A, et al. Pyramidal cells in piriform cortex receive convergent input from distinct olfactory bulb glomeruli. The Journal of neuroscience. 2010; 30:14255–14260. [PubMed: 20962246]
79. Davison IG, Ehlers MD. Neural circuit mechanisms for pattern detection and feature combination in olfactory cortex. Neuron. 2011; 70:82–94. [PubMed: 21482358]
80. Miyamichi K, et al. Cortical representations of olfactory input by trans-synaptic tracing. Nature. 2011; 472:191–196. [PubMed: 21179085]
81. Onoda N, et al. Odor-intensity coding in the anterior piriform cortex. Chem Senses. 2005; 30(Suppl 1):i162–163. [PubMed: 15738092]
82. Sugai T, et al. Odor-concentration coding in the guinea-pig piriform cortex. Neuroscience. 2005; 130:769–781. [PubMed: 15590159]
83. Pause BM, et al. Central processing of odor concentration is a temporal phenomenon as revealed by chemosensory event-related potentials (CSERP). Chem Senses. 1997; 22:9–26. [PubMed: 9056082]
84. Tateyama T, et al. Relation of olfactory event-related potentials to changes in stimulus concentration. Electroencephalogr Clin Neurophysiol. 1998; 108:449–455. [PubMed: 9780015]
85. Rolls ET, et al. Different representations of pleasant and unpleasant odours in the human brain. Eur J Neurosci. 2003; 18:695–703. [PubMed: 12911766]
86. Bensafi M, et al. Neural coding of stimulus concentration in the human olfactory and intranasal trigeminal systems. Neuroscience. 2008; 154:832–838. [PubMed: 18485604]
87. Winston JS, et al. Integrated neural representations of odor intensity and affective valence in human amygdala. J Neurosci. 2005; 25:8903–8907. [PubMed: 16192380]
88. Anderson AK, et al. Dissociated neural representations of intensity and valence in human olfaction. Nat Neurosci. 2003; 6:196–202. [PubMed: 12536208]
89. Johnson, B. Bioengineering. University of California; Berkeley: 2006. Encoding of Olfactory Intensity in Humans; p. 281
90. Zatorre RJ, et al. Neural mechanisms involved in odor pleasantness and intensity judgments. Neuroreport. 2000; 11:2711–2716. [PubMed: 10976949]
91. Li W, et al. Right orbitofrontal cortex mediates conscious olfactory perception. Psychol Sci. 2010; 21:1454–1463. [PubMed: 20817780]
92. Bowman NE, et al. Temporal integration of olfactory perceptual evidence in human orbitofrontal cortex. Neuron. 2012; 75:916–927. [PubMed: 22958830]
93. Seubert J, et al. Orbitofrontal Cortex and Olfactory Bulb Volume Predict Distinct Aspects of Olfactory Performance in Healthy Subjects. Cereb Cortex. 2012
94. Gottfried JA, et al. Remembrance of odors past: human olfactory cortex in cross-modal recognition memory. Neuron. 2004; 42:687–695. [PubMed: 15157428]
95. Price JL. Multisensory convergence in the orbital and ventrolateral prefrontal cortex. Chemosensory Perception. 2008; 1:103–109.
96. Lundstrom JN, et al. Central Processing of the Chemical Senses: an Overview. ACS Chem Neurosci. 2011; 2:5–16. [PubMed: 21503268]
97. Frasnelli J, et al. Neuroanatomical correlates of olfactory performance. Exp Brain Res. 2010; 201:1–11. [PubMed: 19730837]
98. Kjelvik G, et al. The human brain representation of odor identification. J Neurophysiol. 2012; 108:645–657. [PubMed: 22539820]
99. Igarashi KM, et al. Coordination of entorhinal-hippocampal ensemble activity during associative learning. Nature. 2014

100. Frank RA, et al. Assessment of the Sniff Magnitude Test as a clinical test of olfactory function. Physiol Behav. 2003; 78:195–204. [PubMed: 12576116]
101. Duchamp-Viret P, et al. Peripheral odor coding in the rat and frog: quality and intensity specification. J Neurosci. 2000; 20:2383–2390. [PubMed: 10704512]
102. Batsel HL, Lines AJ Jr. Bulbar respiratory neurons participating in the sniff reflex in the cat. Exp Neurol. 1973; 39:469–481. [PubMed: 4712901]
103. Shusterman R, et al. Precise olfactory responses tile the sniff cycle. Nat Neurosci. 2011; 14:1039–1044. [PubMed: 21765422]
104. Uchida N, Mainen ZF. Speed and accuracy of olfactory discrimination in the rat. Nat Neurosci. 2003; 6:1224–1229. [PubMed: 14566341]
105. Rinberg D, et al. Speed-accuracy tradeoff in olfaction. Neuron. 2006; 51:351–358. [PubMed: 16880129]
106. Abraham NM, et al. Maintaining accuracy at the expense of speed: stimulus similarity defines odor discrimination time in mice. Neuron. 2004; 44:865–876. [PubMed: 15572116]
107. Hummel T, Kobal G. Differences in human evoked potentials related to olfactory or trigeminal chemosensory activation. Electroencephalogr Clin Neurophysiol. 1992; 84:84–89. [PubMed: 1370406]
108. Livermore A, et al. Chemosensory event-related potentials in the investigation of interactions between the olfactory and the somatosensory (trigeminal) systems. Electroencephalogr Clin Neurophysiol. 1992; 83:201–210. [PubMed: 1381671]
109. Murphy C, et al. Olfactory event-related potentials and aging: normative data. Int J Psychophysiol. 2000; 36:133–145. [PubMed: 10742568]
110. Jones FN, Woskow MH. On the intensity of odor mixtures. Ann N Y Acad Sci. 1964; 30:484–494. [PubMed: 14220541]
111. Cruz G, Lowe G. Neural coding of binary mixtures in a structurally related odorant pair. Scientific reports. 2013; 3:1220. [PubMed: 23386975]
112. Weiss T, et al. Perceptual convergence of multi-component mixtures in olfaction implies an olfactory white. Proc Natl Acad Sci U S A. 2012; 109:19959–19964. [PubMed: 23169632]
113. Carmichael ST, et al. Central olfactory connections in the macaque monkey. J Comp Neurol. 1994; 346:403–434. [PubMed: 7527806]
114. Price, JL. The olfactory system. In: Paxinos, G., editor. The human nervous system. Academic; 2003. p. 1198-1212.
115. Reisert J, Matthews HR. Adaptation of the odour-induced response in frog olfactory receptor cells. The Journal of physiology. 1999; 519(Pt 3):801–813. [PubMed: 10457092]
116. Hamilton KA, Kauer JS. Patterns of Intracellular-Potentials in Salamander Mitral Tufted Cells in Response to Odor Stimulation. J Neurophysiol. 1989; 62:609–625. [PubMed: 2549211]
117. Tan J, et al. Odor information processing by the olfactory bulb analyzed in gene-targeted mice. Neuron. 2010; 65:912–926. [PubMed: 20346765]

Box 2

Open questions

- Can perceived intensity be predicted from molecular structure?
- Can any models predict mixture intensity, when the component concentration-intensity functions are known? If mixture components (or sub-qualities) are identifiable, do they have independent intensities (i.e. is intensity multichannel data?)
- Can any models predict intensity across odors?
- Can any models predict perceptual adaptation—how perceived intensity decreases over time with continuous stimulus presentation?
- How is intensity ultimately represented, computed or read by neural circuits, at the level of perceived odor sensation? Do any of the concentration codes generated in earlier or later stages of the pathway contribute to this final intensity representation?

Highlights

- Olfaction lacks a working model of odor intensity coding.
- Neural correlates of varying odor concentration lead to simplistic models.
- New models are needed that predict intensity across odors, in mixtures, and after adaptation.

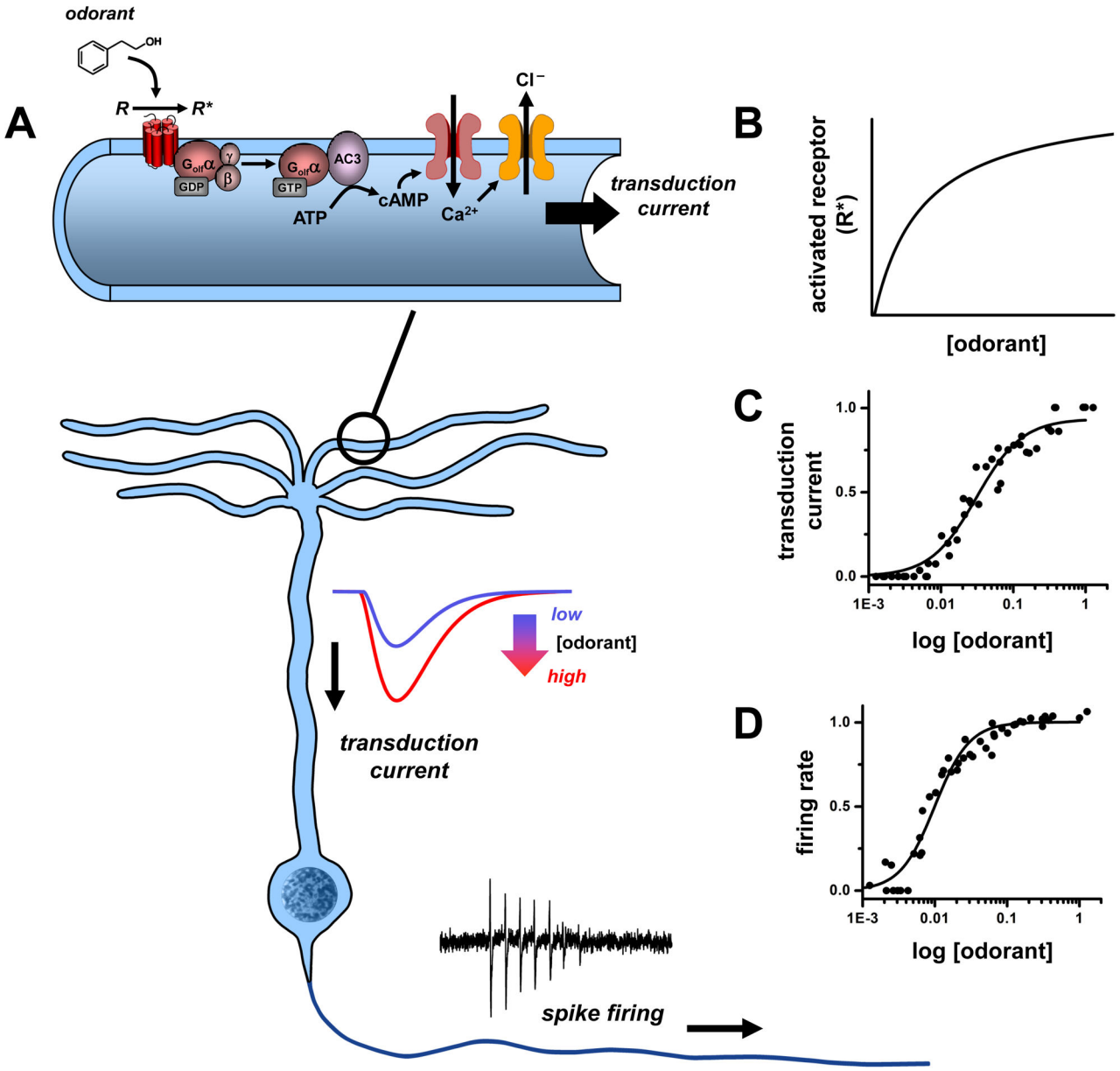

Figure 1. Odorant concentration coding in olfactory sensory neurons (OSNs)

During sensory transduction (**A**), odorant molecules bind and stabilize the active states of olfactory receptors (R) in ciliary membranes of OSNs. The activated receptors (R*) couple to G-proteins (G_{olf}) and increase synthesis of cyclic AMP (cAMP) by type III adenylyl cyclase (AC3). The cAMP opens cyclic nucleotide-gated channels that conduct calcium ions into the cilia and in turn open a channel (ANO2) mediating a depolarizing efflux of chloride ions. The resulting transduction current is passed to the OSN cell body where it drives a train of action potentials (spikes). The concentration of detected odorant is encoded non-linearly at each step of transduction: by a hyperbolic dependence on the number of activated receptors (R*) in the cilia (**B**), a strongly cooperative variation in amplitude of the transduction current (**C**), and similar sigmoidal variation of spike firing rate relayed by OSN

axons (**D**). Data source: **C, D:** [115], normalized currents and firing rates of frog OSN response to cineole; mammalian OSNs exhibit similar dose-response profiles.

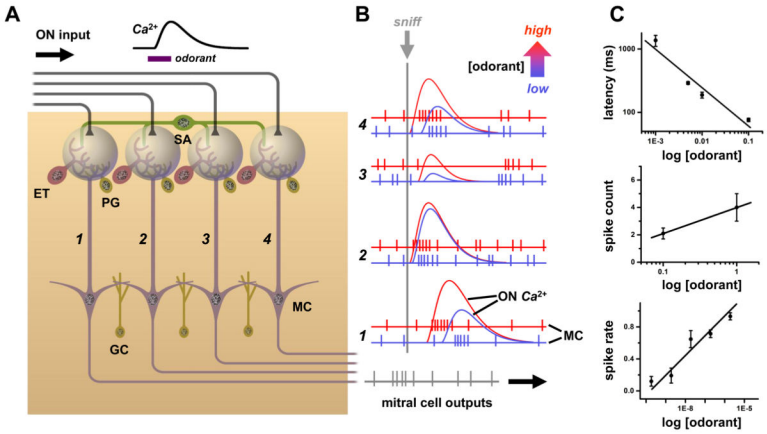

Figure 2. Spatial and temporal coding of odorant concentration in the olfactory bulb

A. Schematic of four parallel glomerular odor-encoding channels. During responses to odorant stimuli sampled by a single sniff, olfactory nerve (ON) spike inputs to different glomeruli exhibit different latencies and time courses (monitored by calcium indicator fluorescence signals). This reflects the diversity of olfactory receptor molecular tunings. These spatiotemporal patterns of input are processed by glomerular neural circuits, including excitatory external tufted (ET), as well as inhibitory periglomerular (PG) and short axon (SA) cells, before being encoded into spiking patterns of mitral cells (MC) for relay to olfactory cortex. The SA cells have widespread interglomerular projections that could act to normalize spatial patterns of glomerular output as input patterns vary with odorant concentration (c.f. Fig. 5B). A second layer of signal filtering and pattern transformation occurs when granule cells (GC) or other local interneurons inhibit mitral cells. **B.** As odorant concentration is increased from low (blue) to high (red), OSNs are activated more rapidly and presynaptic glomerular responses have shorter latencies (c.f. red ON traces). Mitral cell spike output may track these latency shifts over the sniff cycle (c.f. left-shifted red spike responses in glomerular channels 1, 3 & 4). Such phase shifts of spike latency over sniff cycles may encode odor concentration, while leaving invariant overall patterns of relative latencies between glomeruli (which can encode odor quality, as latencies will vary with different sensitivities of receptors to different odorants). This simple scheme allows early separation of the coding of odor concentration vs. odor quality, but may be complicated by lateral inhibition between glomeruli. Some mitral cells exhibit suppressed basal spiking in response to an odor, which may be followed by rebound spiking whose latency becomes longer as odorant concentration is increased (due to stronger inhibition) (as pictured in glomerular channel 2). **C.** Example of excitatory mitral cell response in a glomerular coding channel. Data show a logarithmic decrement of mitral cell spike latency with increasing concentration, which provides an immediate readout of intensity (upper panel). Mitral cell spike count and mean spike rate over a sniff (middle and lower panels) increase, so spike rate coding of concentration is possible if readouts have longer integration times. Data sources: **C**: *upper panel*: [116], salamander mitral/ tufted cell excitatory response to isoamyl acetate; *middle panel*: [41], mean spikes per sniff cycle for rat mitral/ tufted cell response to cineole; *lower panel*: [117], mouse mitral/ tufted cell spike response evoked by heptanal activation of olfactory receptor I7 (mean of 8 cells, spike rate increment over baseline rate, normalized to maximum rate).

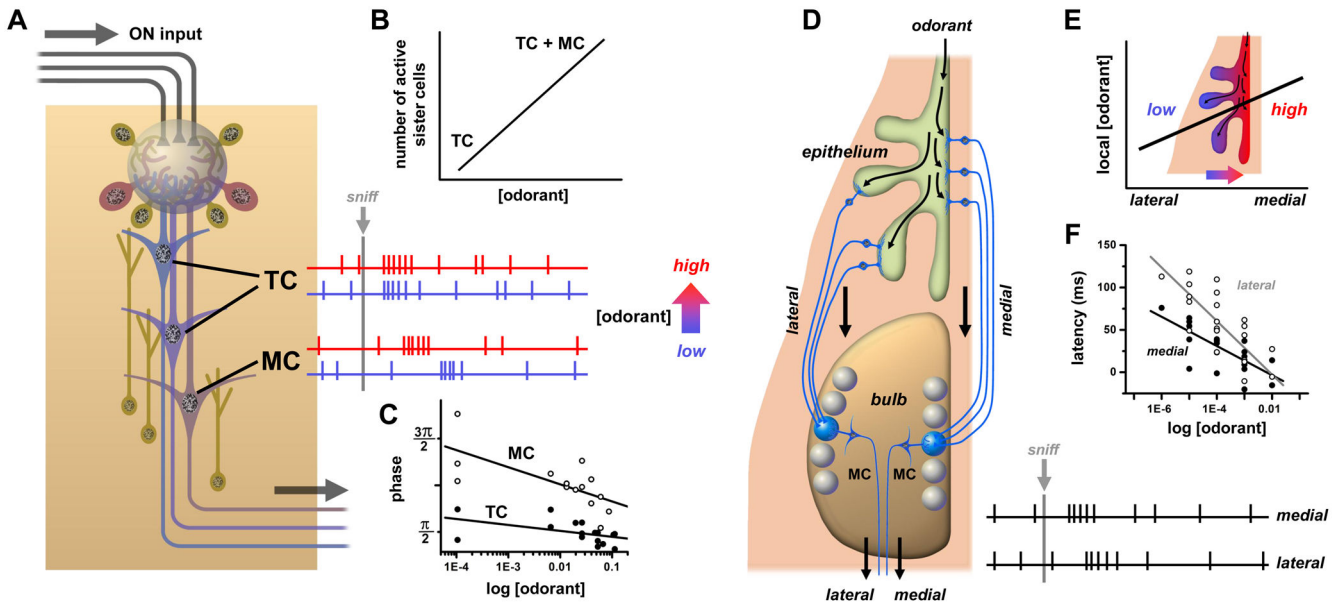

Figure 3. Odorant concentration coding in glomerular circuits

A. Each glomerulus transforms the afferent ON signals transduced by one type of olfactory receptor into the spike activities of several dozen or more mitral cells (MC) and tufted cells (TC). The two classes (MC, TC) of olfactory bulb output neurons differ in connectivity and regulation by local circuits. Various subtypes of tufted cells are located more superficially, receive more direct ON input and less granule cell inhibition, and are more easily excited. The mitral cells are located deeper, receive mostly indirect ON input (via ET cells) and more granule cell inhibition, and have higher spike thresholds. **B.** Coding of odorant concentration by the number or fraction of responding 'sister' mitral/ tufted (i.e. connected to the same glomerulus). When odorant concentration is increased, stronger afferent ON input to the glomerulus can recruit a greater proportion of sister mitral/ tufted cells, including those with higher spike thresholds. **C.** Coding of odorant concentration by shift in spike latency between mitral and tufted cells. When odorant concentration is increased (blue to red traces), latency and sniff cycle phase of mitral cell spike responses decreases while that of tufted cells remains approximately invariant. **D.** Coding of odorant concentration by medio-lateral timing difference in activation of pairs of glomeruli corresponding to the same olfactory receptor. Inhaled odorant gains access to OSNs in medial olfactory epithelium (on septum) sooner than OSNs in lateral olfactory epithelium (in recesses of nasal turbinates). This results in a latency difference between inputs to glomeruli of mirror image receptor maps in medial and lateral halves of the olfactory bulb. **E.** Medio-lateral gradient in concentration at fixed time due to relative lag in odorant access. This gradient may depend on sorption properties of the odorant. **F.** As odorant concentration is increased, the latency of spike responses drops at different rates for mitral cells connected to medial vs. lateral glomeruli. Data sources: **C**: [46], average spike phase of mouse mitral cell vs. tufted cell response to various odorants; **F**: [49], onset latencies of mitral cell spike responses in medial vs. lateral olfactory bulb of transgenic mice with expression of olfactory receptor I7 in all OSNs activated by octanal.

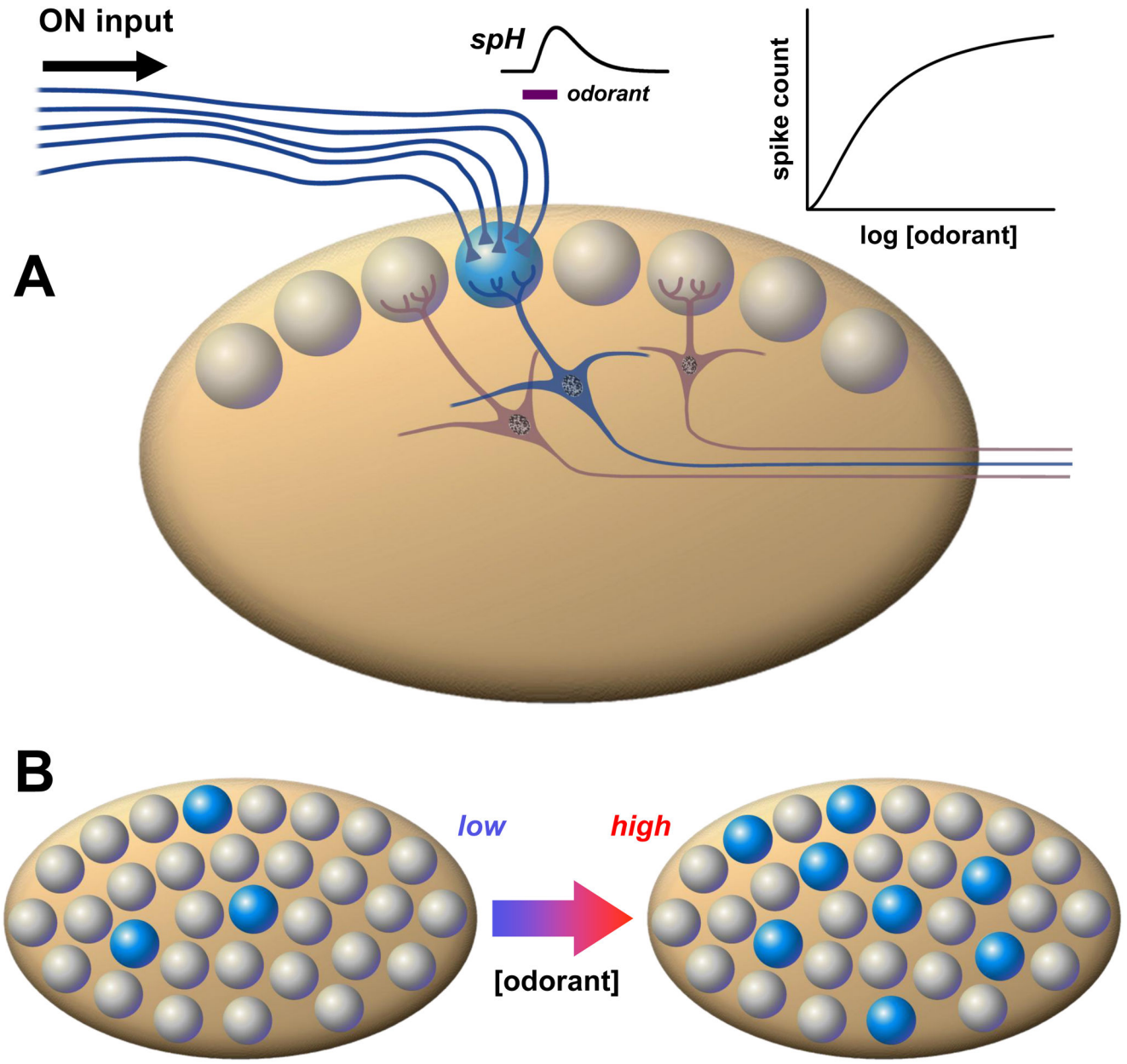

Figure 4. Odorant concentration coding in olfactory bulb glomeruli

A. Thousands of OSNs expressing the same olfactory receptor relay convergent synaptic input via the olfactory nerve (ON) to one or a few glomeruli at stereotypic locations in the olfactory bulb. The collective inputs to individual glomeruli can be quantified by optical measurements of odorant responses using presynaptic indicators of calcium signaling, or transmitter release (e.g. the exocytosis reporter synaptopHluorin, *spH*). This reveals coding of odorant concentration by a weakly cooperative dose- response curve. **B.** Each glomerulus receives input from one type of receptor out of a diverse population of ~ 10^2 – 10^3 different receptors, with different odorant tunings. This means that as concentration of a particular odorant increases, a large set of receptors (and hence glomeruli) is recruited. This spatial

expansion of the number of activated glomeruli (shown here in blue) has been suggested to serve as a concentration code at the system level.